

Damage and Recovery of the Bone Growth Mechanism in Young Rats Following 5-Fluorouracil Acute Chemotherapy

Cory J. Xian,* Johanna C. Cool, Tim Pyragius, and Bruce K. Foster

Department of Orthopaedic Surgery, University of Adelaide Department of Paediatrics, Women's and Children's Hospital, North Adelaide, South Australia

Abstract Chemotherapy-induced bone growth arrest and osteoporosis are significant problems in paediatric cancer patients, and yet how chemotherapy affects bone growth remains unclear. This study characterised development and resolution of damage caused by acute chemotherapy with antimetabolite 5-fluorouracil (5-FU) in young rats in the growth plate cartilage and metaphyseal bone, two important tissues responsible for bone lengthening. In metaphysis, 5-FU induced apoptosis among osteoblasts and preosteoblasts on days 1–2. In growth plate, chondrocyte apoptosis appeared on days 5–10. Interestingly, Bax was induced prior to apoptosis and Bcl-2 was upregulated during recovery. 5-FU also suppressed cell proliferation on days 1–2. While proliferation returned to normal by day 3 in metaphysis, it recovered partially on day 3, overshoot on days 5–7 and normalised by day 10 in growth plate. Histologically, growth plate heights decreased by days 4–5 and returned normal by day 10. In metaphysis, primary spongiosa height was also reduced, mirroring changes in growth plate thickness. In metaphyseal secondary spongiosa, a reduced bone volume was observed on days 7–10 as there were fewer but more separated trabeculae. Starting from day 4, expression of some cartilage/bone matrix proteins and growth factors (TGF- β 1 and IGF-I) was increased. By day 14, cellular activity, histological structure and gene expression had returned normal in both tissues. Therefore, 5-FU chemotherapy affects bone growth directly by inducing apoptosis and inhibiting proliferation at growth plate cartilage and metaphyseal bone; after the acute damage, bone growth mechanism can recover, which is associated with upregulated expression of matrix proteins and growth factors. *J. Cell. Biochem.* 99: 1688–1704, 2006. © 2006 Wiley-Liss, Inc.

Key words: chemotherapy; bone growth arrest; osteoporosis; growth plate; side effects; 5-FU

Bone lengthening is achieved through a process called endochondral ossification at the growth plate cartilage and its adjacent metaphyseal bone towards the ends of long bones. In this process, a cartilaginous template is made at the growth plate and then it is replaced by bone at the metaphysis. This complex sequence of morphological and biochemical changes is

initiated when cells at the growth plate resting zone are activated to proliferate at the proliferative zone and then proceed through maturation at the hypertrophic zone [Ianotti, 1990]. Simultaneously, chondrocytes produce a matrix that undergoes mineralisation at the hypertrophic zone and later die by apoptosis at the growth plate-metaphysis transitional zone. The mineralised cartilage is invaded by blood vessels, which bring in bone forming cells (osteoblasts) that synthesize bone-matrix on trabecular surface of calcified cartilage/bone, and resorptive cells (osteoclasts) that resorb and thus remodel the mineralised cartilage or bone to trabecular bone with bone marrow at the metaphysis.

Endochondral bone growth activity is controlled by many genetic factors, including hormones, growth factors, cytokines, their receptors and transcriptional factors. For example, insulin-like growth factor (IGF-I) is a survival and mitogenic factor for both chondrocytes and

This article has been changed online since its original publication on August 3, 2006 in Wiley Interscience. Tim Pyragius has been added as an author of the article.

Grant sponsor: Bone Growth Foundation (South Australia); Grant sponsor: National Health and Medical Research Council of Australia.

*Correspondence to: Dr. Cory J. Xian, Department of Orthopaedic Surgery, Women's and Children's Hospital, 72 King William Road, North Adelaide, SA 5006 Australia. E-mail: cory.xian@adelaide.edu.au

Received 9 January 2006; Accepted 11 January 2006

DOI 10.1002/jcb.20889

© 2006 Wiley-Liss, Inc.

osteoblasts and a differentiation factor for osteoblasts [Sims et al., 2000; Yakar and Rosen, 2003], and transforming growth factor-beta (TGF- β 1) is an important mitogenic factor for chondrocytes and a differentiation factor for bone cells [Price et al., 1994]. Mature osteoblasts, located on the surface of calcified cartilage trabeculae or metaphyseal trabecular bones, are derived from the stromal osteoprogenitor cells of bone marrow [Beresford, 1989]. Under influence of signals such as IGF-I and TGF- β , osteoprogenitor cells first transform to the transitional preosteoblasts which further differentiate to osteoblasts [Kember, 1993; Long, 2001]. Osteoclasts are produced from the marrow haematopoietic pathway; and upon activation, they bind to the surface of calcified tissues, and secrete acid and proteolytic enzymes to undergo resorption [Marks, 1998].

Endochondral bone growth activity is also affected by environmental factors such as nutrition and medical treatments including chemotherapy. In recent years due to the more successful but highly intensive chemotherapy regimens used to treat childhood and adult cancers, there has been a significant increase in chronic toxicity to normal tissues including bone in cancer patients [Linet et al., 1999]. Chemotherapy, usually with combinations of anticancer agents with an anti-metabolite [Peters et al., 2000], is commonly the first line strategy for the treatment of cancers, particularly in children in whom radiotherapy is often contraindicated due to its long-term detrimental effects [Clayton et al., 1988]. Short stature, osteoporosis, bone pain and fractures are important skeletal side effects in paediatric chemotherapy patients and in adult survivors. Studies showed that a decrease in height growth velocity occurred in 73% of acute lymphoblastic leukaemia (ALL) patients at 12 months of chemotherapy [Halton et al., 1998], and intensive chemotherapy for ALL adversely affects lower leg growth particularly in the first few weeks of therapy [Ahmed et al., 1999], and during periods of intensive chemotherapy [Crofton et al., 1998; Mushtaq and Ahmed, 2002]. Depending on chemotherapy regimens, patterns of growth after cessation of treatment vary, with some studies reporting a permanent deficit [Schriock et al., 1991; Caruso-Nicoletti et al., 1993], whereas others revealing catch-up growth to a certain extent [Glasser et al., 1991; Ahmed et al., 1997]. Consistently, experimental

studies in rats found that methotrexate, cisplatin or doxorubicin also significantly reduced bone growth [Friedlanender et al., 1984; van Leeuwen et al., 2000a].

Childhood leukaemia survivors are also at risk of a reduced bone density, and clinical studies have highlighted osteoporosis as a complication of chemotherapy for childhood malignancy [Halton et al., 1996; Mushtaq and Ahmed, 2002]. This osteoporotic condition increases bone fracture risk with a fracture incidence during leukaemia treatment as high as 39% [Mushtaq and Ahmed, 2002], and the poor bone quality persists into adult life and may increase bone fracture risk at an older age [van Leeuwen et al., 2000b]. Due to the trend of further intensification of chemotherapy and improved survival rates in paediatric cancer patients, understanding the bone growth arrest and osteoporosis side effects is important.

Despite the large number of clinical reports that describe the effects of chemotherapy on skeletal growth and bone density, only a few studies have examined aspects of potential mechanisms by which chemotherapy affects bone formation and growth. Children treated with chemotherapy alone show no disturbance in growth hormone secretion [Samuelsson et al., 1997], suggesting that effects of chemotherapy on bone growth are independent of the hypothalamic-pituitary axis [Siebler et al., 2002]. Since chemotherapeutic agents can elicit cellular responses including growth arrest and apoptotic cell death, disturbances in skeletal growth result when there is a disruption of normal activity and their progenitor cell supply of growth plate chondrocytes, bone-forming osteoblasts and bone/cartilage remodelling osteoclasts. Using an acute chemotherapy model in young rats with anti-metabolite 5-fluorouracil (5-FU), our earlier study showed that a single injection of 5-FU caused rapid and significant suppression in cell proliferation in the growth plate and metaphysis and induction of apoptosis in the metaphysis, thus providing *in vivo* evidence that 5-FU chemotherapy impairs the bone growth mechanism directly to reduce longitudinal bone growth [Xian et al., 2004a]. 5-FU exerts its anti-cancer effects through inhibition of thymidylate synthase, an enzyme required for the synthesis of thymine nucleotide, and incorporation of its metabolites into RNA and DNA [Longley et al., 2003]. 5-FU is used in treatment of solid tumours not only in

adult cancer patients (with colorectal or breast cancers or cancers of the aerodigestive tract) [Peters et al., 2000; Longley et al., 2003], but also used in treating childhood solid tumours, including head and neck cancers, hepatoblastoma, colon cancer, nasopharyngeal carcinoma, esophageal/gastric junction adenocarcinoma, glioma and skin cancer [Kim et al., 1989; Angel et al., 1992; Zidan et al., 1997; Saade et al., 1999; Sasaki et al., 1999; Snir et al., 2000; Katzenstein et al., 2003].

To examine how well the bone growth mechanism can recover after chemotherapy insult and to study potential molecular mechanisms underlying these changes, using the 5-FU acute chemotherapy model in young rats [Xian et al., 2004a], the current study characterised acute 5-FU treatment-induced development and resolution of the defects in growth plate and metaphysis by examining the changes in cell apoptosis and proliferation, changes in histological structures and alteration in expression of matrix molecules and some regulatory molecules known to be important in regulating the above cellular processes in the growth plate and metaphysis, the two most important tissues for bone growth.

MATERIALS AND METHODS

Rat 5-FU Chemotherapy Trial and Specimen Collection

Fifty-four male Sprague–Dawley young rats (6 weeks old) were randomly allocated into 9 groups ($n=6$), and received a single intraperitoneal injection of 150 mg/kg 5-FU as we have previously described [Xian et al., 2004a]. To observe time-course injury and recovery responses, groups of rats were culled by CO₂ overdose for specimen collection on days 1–5, 7, 10 and 14 after the 5-FU injection. One group of rats ($n=6$) received saline injection was used as a normal control group and were culled on day 14. During the course of the trial, the rat body weights were recorded daily. Ninety minutes prior to sacrifice, rats were injected with 50 mg/kg of thymidine analogue 5'-bromo-2'-deoxyuridine (BrdU) (Sigma, NSW, Australia) to label S-phase nuclei for studies of cell proliferation. For the day-14 time-point groups, the total body lengths of rats (from the tip of nose to the end of the tail) were measured at the time of 5-FU injection and at sacrifice. The protocol followed the Australian Code of Practice for the Care and

Use of Animals and was approved by the Animal Ethics Committee of Women's and Children's Hospital, South Australia.

After sacrifice, tibiae were dissected free of soft tissues and the length of the left tibia was measured. Growth plate cartilage from the left proximal tibia was collected by scraping using a fine blade, and metaphyseal bone of 3-mm in length was sawed off using a fine saw from the proximal metaphyseal end of the left tibia, and were frozen in liquid nitrogen and stored at -80°C for RNA extraction purpose. The right proximal tibia containing the growth plate and 1-cm adjacent bone was collected, fixed in 10% buffered formalin for 24 h and decalcified in 14% EDTA for 2 weeks at 4°C . The tibial specimens were bisected longitudinally using a fine scalpel blade, with one half being processed routinely and embedded in paraffin wax. Paraffin sections of 5- μm thick were cut and mounted on positively-charged SuperFrost PlusTM coated glass slides for histological and immunohistochemical studies.

In addition, for generating undecalcified sections, one more normal group ($n=6$) and one more 5-FU-injected group ($n=6$) were similarly set up and were sacrificed on day 14, with their left proximal tibiae collected, fixed in formalin and processed routinely for methyl-methacrylate resin embedding.

Histomorphometric Analysis of Growth Plate and Metaphysis

Histology staining. To visualise bone, growth plate cartilage and their histology structures, alcian blue haematoxylin and eosin (H&E) histological staining was performed. Briefly, dewaxed and rehydrated sections were stained in 0.3% alcian blue in 3% acetic acid (pH 2.5) for 40 min, followed by rinse and routine H&E staining. In addition, undecalcified sections were stained routinely with von Kossa and H&E.

Growth plate zonal thickness and metaphyseal heights. As an analysis of chemotherapy effects on structural changes in growth plate cartilage and metaphyseal bone, alcian blue H&E-stained sections were used for morphometric measurements of growth plate zonal thickness, heights of primary and secondary spongiosa, and areas of trabecular bone at the metaphyseal bone using an image analysis system with the Image Pro Plus software (Media Cybernetics, Silver Springs, MD) [Xian

et al., 2004a]. Under a 20× objective, the average zonal heights of the growth plate cartilage was obtained by measuring heights of the resting, proliferative and hypertrophic zones of the entire growth plate section along an axis oriented 90° to the transverse plane of the growth plate and parallel to the longitudinal axis of the tibial bone [Sanchez and He, 2002]. Similarly, the average primary and secondary spongiosa zonal heights at the metaphysis were measured using the same software. While the trabecular complexes in the primary spongiosa are basically trabeculae of calcified cartilage core covered by a layer of newly synthesised bone lined by a layer of osteoblasts, the secondary spongiosa is a region where the bone trabeculae from primary spongiosa are further remodelled to become thicker in size and fewer in number.

Measurements of trabecular numbers, thickness, spacing and bone volume. To examine potential treatment effects on bone formation, histomorphometric measurements were also conducted at both the primary and secondary spongiosa to examine chemotherapy effects on trabecular number, thickness, spacing and bone volume fraction (bone volume/total tissue volume) as described [Fazzalari et al., 1997; Byers et al., 2000; Xian et al., 2004a]. Within the primary spongiosa at a position 0.1 mm above the primary-secondary transitional zone, a transverse line was drawn across the metaphysis, and the numbers and transverse thickness of intercepting trabeculae, as well as the transverse distance or spacing between these trabeculae were measured. Similarly, within the secondary spongiosa at a position 1 mm below the transitional zone, the above measurements were made. In addition, at similar regions within the primary and secondary spongiosa, all the trabeculae complexes were traced, and their areas as well as the total tissue areas were measured, which were then used to calculate the bone volume fraction (area of the trabecular complexes/total primary or secondary spongiosa area) (%).

Numbers of chondrocytes per column and osteoblasts/pre-osteoblasts and osteoclasts on trabecular surface. Numbers of chondrocytes per column at the growth plate proliferative and hypertrophic zones were counted as described [Xian et al., 2004a]. All well-orientated “full or intact” cell columns (i.e., columns sectioned in a plane showing consecu-

tive cells extending the entire thickness of each zone) were included for the analysis, and the numbers of cells residing within the proliferative and hypertrophic zones in these columns were counted, expressed as numbers of cells per column.

Similarly, on the trabecular surface at the primary and secondary spongiosa, numbers of osteoblasts and pre-osteoblasts along the perimeter were counted and expressed as numbers of cells per length of perimeter (cells/mm). Osteoblasts are cuboidal in shape and line the trabecular surfaces in location, while pre-osteoblasts are functionally defined as a transitional state between the osteoprogenitor cells and the differentiated osteoblasts, and are morphologically defined as spindle-like cells located between the juxtatrabecular osteoblast layer and the bone marrow [Hoshi et al., 1997].

Osteoclasts are multinuclear cells responsible for resorbing calcified cartilage or bone trabeculae. On alcian blue-H&E stained sections, cells having at least three nuclear profiles and apposing trabecular surface with an active resorption front [Damron et al., 2003] were counted and expressed as cells/mm trabecular perimeter length within primary spongiosa and secondary spongiosa.

BrdU Labelling and Measurement of Labelling Indices

To examine effects of 5-FU treatment on proliferation of chondrocytes and bone cells, paraffin sections were used for BrdU labelling using a monoclonal antibody (Dako, Carpinteria, CA) as described [Xian et al., 1999; Xian et al., 2004b]. In the growth plate, numbers of BrdU-positive cells and the total numbers of chondrocytes within the proliferative zone were counted to calculate the BrdU labelling index (%) [Xian et al., 2004a]. In the metaphyseal primary and secondary spongiosa regions, the total numbers of osteoblasts and pre-osteoblasts and the BrdU-labelled osteoblasts/pre-osteoblasts were counted along the perimeter surface of the trabeculae, and expressed as numbers of BrdU labelled cells per unit length (mm) of trabecular surface [Xian et al., 2004a].

Hoechst and TUNEL Apoptosis Staining and Density Measurement of Apoptotic Cells

To assess the effects of 5-FU treatment on apoptotic cell death, cell nuclear morphology

staining was conducted using fluorescent Hoechst dye (Molecular Probes, Eugene, OR) as described [Xian et al., 2004a], and terminal deoxynucleotidyl transferase dUTP nick end labelling (TUNEL) reaction (Roche Biochemicals, NSW, Australia) was performed as described [Xian et al., 2002, 2004a]. Furthermore, morphology and location of the apoptotic cells were also examined on sections with alcian blue-H&E histology staining which reveal characteristic apoptotic features of nuclear fragmentation and cytoplasmic condensation.

The density of apoptotic cells (identified by Hoechst dye staining) was measured at proliferative zone of the growth plate (chondrocytes) and at the primary spongiosa (both osteoblasts and preosteoblasts). The total numbers of apoptotic cells and the total areas of growth plate proliferative zone and metaphyseal primary spongiosa were then used to calculate the apoptotic cell density (cells/mm²) as described [Xian et al., 2004a].

Real Time RT PCR

To examine changes in gene expression during 5-FU acute chemotherapy-induced injury and repair, relative mRNA expression levels were measured in RNA samples from growth plate and metaphysis for the following genes: growth factors IGF-I and TGF- β 1, apoptosis regulatory molecules Bcl-2 (anti-apoptotic) and Bax (pro-apoptotic), and major matrix proteins in the growth plate (collagen-2 and collagen-10) and bone (collagen-1 and osteocalcin). Total RNA from frozen growth plate cartilage and metaphyseal bone was extracted and purified [Zhou et al., 2004]. Due to the small amounts of RNA that can be isolated from rat growth plate and the numbers of genes that need to be assays, purified total RNA from the 6 rats in each time point group were pooled to obtain a total of 5 μ g RNA. cDNA was then synthesised from the pooled RNA samples using

random decamers (Geneworks, Australia) and Superscript-II RNase H-reverse transcriptase (Stratagene, USA) as described [Zhou et al., 2004]. Qiagen QuantiTect™ SYBR® Green PCR assays for each target molecule and internal reference Cyclophilin A were then performed using specific primers (Table I) in parallel in three replicates on these cDNA samples, using a Rotorgene 72-well PCR machine (Corbett Research, NSW, Australia) [Zhou et al., 2004]. From the amplification curves generated, the initial amount of gene transcript of the target gene (R_0) was normalised to that of Cyclophilin A for each sample as described [Liu and Saint, 2002; Zhou et al., 2004], and the expression levels of the target gene after 5-FU treatment were expressed as folds of the expression level of the normal rat control group.

Statistics

Measurements are presented as mean \pm SEM and were analysed by a one-way analysis of variance (ANOVA). When the significance levels ($P < 0.05$) were achieved, a post-hoc analysis of groups was performed using a Tukey's test. In the figures, the symbols *, ** and *** represent $P < 0.05$, $P < 0.01$ and $P < 0.001$, respectively.

RESULTS

Effects of 5-FU on Body Growth

One single dose of 5-FU considerably decreased the body weight gain of the treated rats compared to normal rats, with the differences in body weights being statistically significant from days 4 to 14 and the treated rats having a 19% smaller body weight by day 14 (Fig. 1A). By day 14, there was also a significantly smaller body length increase in treated rats (average 5.8 cm) compared to controls (average 7.1 cm) ($P < 0.05$) (Fig. 1B), although there was only a slightly shorter tibial bone in the treated animals

TABLE I. Primer Sequences used for Real-Time RT-PCR Analysis

Gene	Forward primer (5'-3')	Reverse primer (5'-3')
IGF-I	CTACAAGTCAGCTCGTTCCATCC	GGTCTTGTTTCCTGCACTTCCTC
TGF- β 1	GGTGGACCGCAACAACGCAATCTA	CTGGCACTGCTTCCCGAATGTCTG
Bcl-2	CAGCATGCGACCTCTGTTTG	TCTGCTGACCTCACTTGTGG
Bax	CGAGAGGTCTTCTTCGCTGT	GAGCACCAGTTTGCTAGCAA
Col-2a	GGGCTCCCAGAACATCACCTACCA	TCGGCCCTCATCTCCACATATTG
Col-10	GGCAGCAGCACTATGACCCAAGAT	ACAGGCCTACCCAAACGTGAGTCC
Col-1	CCCCAAAGACACAGGAAATAATG	GAAGGTGCTGGGTAGGGGAAGTAA
Osteocalcin	GCTGGCCCTGACTGCATTCTG	ATTACCACCTTACTGCCCTCTG
Cyclophilin-A	CGTTGGATGGCAAGCATGTG	TGCTGGTCTTGCCATTCTG

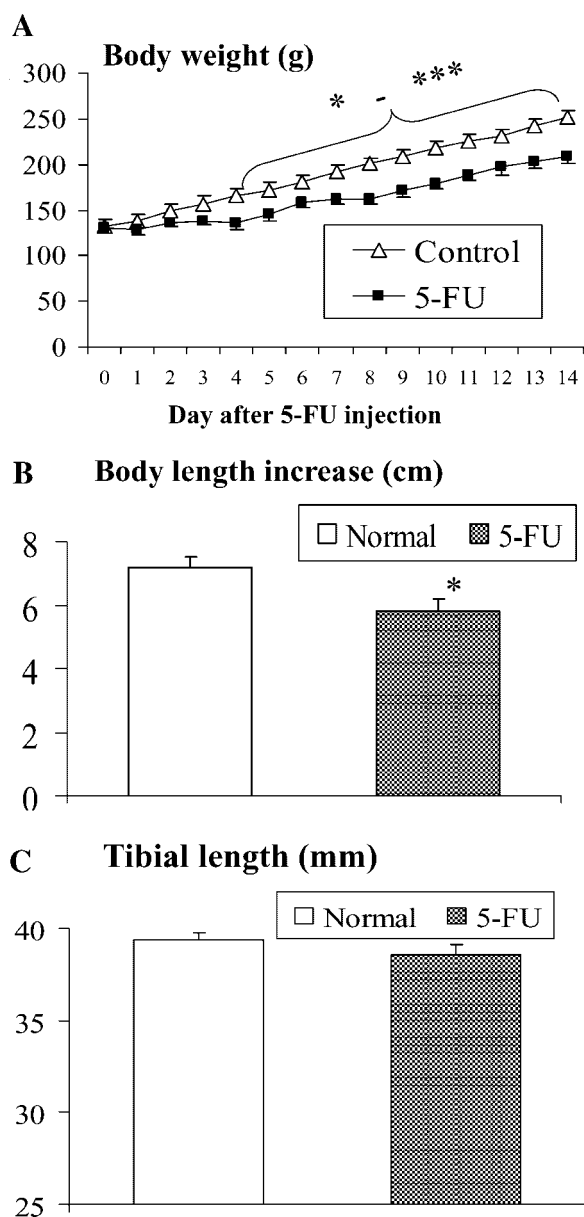


Fig. 1. Effects of a 5-FU single injection (in comparison with saline injection control) on measurements of body weight (A), total body length increase (B), and tibial length (C) within 2 weeks ($n = 6$ rats per group per time point).

(average 38.6 mm) compared to the normal controls (39.3 mm) (Fig. 1C). Our recent study has shown that one single 5-FU injection at the same dosage did not significantly affect the total food and water intakes and the urine output [Cool et al., 2005], suggesting that changes in growth after 5-FU injection resulted from direct effects of 5-FU on body growth rather from a reduced food intake.

Cellular and Histological Structural Changes in the Growth Plate

Growth plate functions to produce a calcified cartilaginous template for bone lengthening. In the present study, we examined the development and resolution of cellular and structural changes in the proximal tibial growth plate of young rats within a 2-week time course after 5-FU injection.

Apoptosis in the growth plate. Administration of 5-FU did not produce obvious effects on apoptosis among cells in the resting and hypertrophic zones of the growth plate over the 2-week time course. While apoptosis can be identified at the lower hypertrophic zone on H&E sections in both normal and 5-FU-treated animals, the apoptotic rate at the hypertrophic zone was not increased by the 5-FU treatment (data not shown). In the proliferative zone, however, administration of 5-FU induced obvious apoptotic cell death among chondrocytes, as examined by nuclear staining with Hoechst dye (Fig. 2A vs. B), with the apoptosis being apparent on day 5, peaking to a statistically significant level on day 7 ($P < 0.001$), declining on day 10 and returning to normal on day 14 (Fig. 2C).

Cell proliferation in the growth plate. In the normal growth plate, as observed in our previous study [Xian et al., 2004a], proliferative activity (as revealed by BrdU labelling within 90 min after a bolus injection of BrdU prior to sacrifice) was detected in the proliferative zone (Fig. 3A) with a labelling index of 11% (Fig. 3C). After 5-FU injection, cell proliferation at the growth plate was dramatically (although statistically insignificantly) suppressed on day 1 (Fig. 3B) and day 2, partially recovered on day 3, recovered on day 4 and slightly overshoot on days 5 and 7, and returned to normal on day 10 (Fig. 3C).

Structural changes at the growth plate. Despite minimal distortion in cellular columnation and morphology, examination of alcian blue-H&E stained sections of proximal tibiae revealed time-course changes in the thickness of the growth plate, with the thinning of growth plate being most obvious on days 3–5 (Fig. 4A vs. B,C), followed by returning to normal by days 10 and 14 (Figs. 4C and 8A vs. D). Detailed histomorphometric measurements reveal a gradual decrease in growth plate thickness, reaching a 26% reduction by days 4 and 5

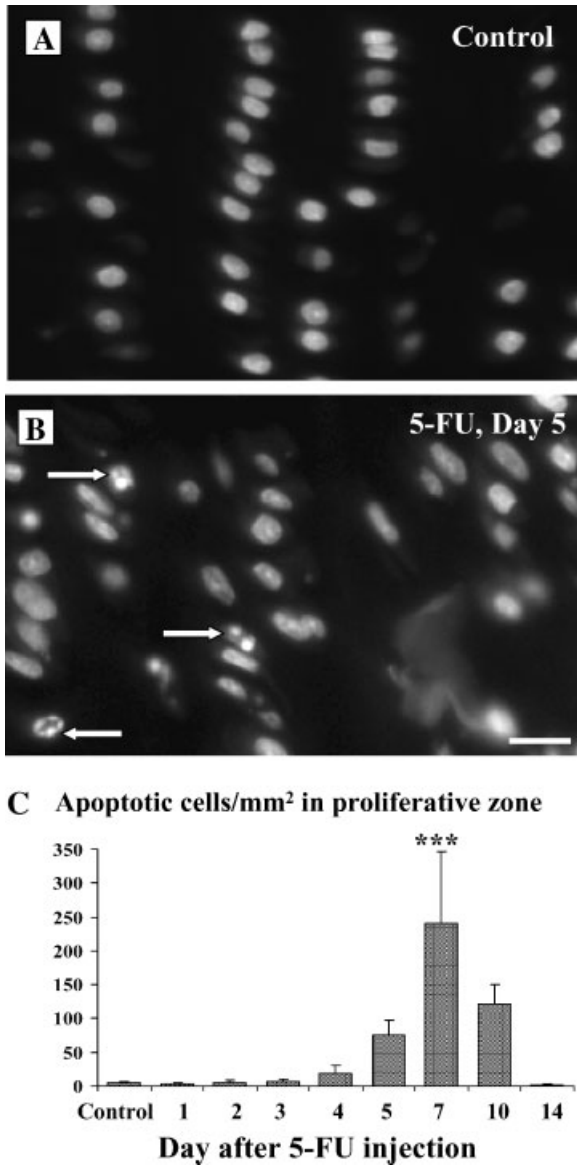


Fig. 2. Apoptosis induction in the growth plate after a single high dose of 5-FU. **A:** A Hoechst dye-stained normal rat growth plate section showing no apoptosis in the proliferative zone. **B:** A Hoechst dye-stained growth plate section of a rat 5 day after 5-FU injection, showing apoptosis in the proliferative zone (arrows). **C:** Density measurements of apoptotic chondrocytes per unit area of the proliferative zone of growth plate. Bar in B = 12.5 μ m (also applies to A).

($P < 0.05$) prior to gradual recovery to the normal thickness around 500 μ m by days 10 and 14 (Fig. 4C). Interestingly, while the thickness of the resting zone was not altered (data not shown), changes in zonal heights of both the proliferative (Fig. 4D) and hypertrophic (Fig. 4E) zones paralleled the changes in total growth plate thickness (Fig. 4C), suggesting that 5-FU treatment reduced growth

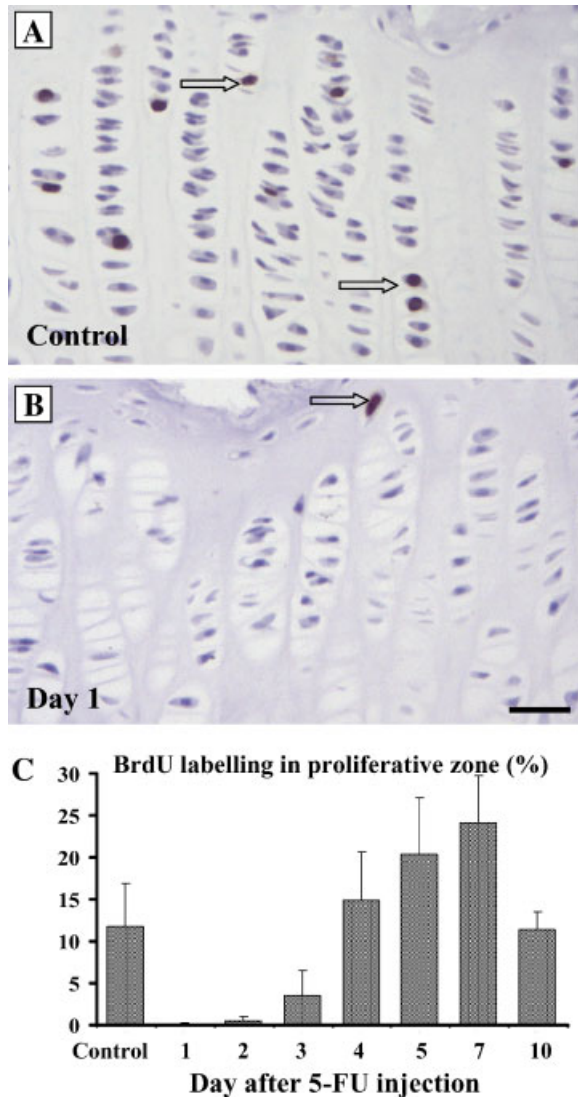


Fig. 3. Suppression and recovery of BrdU labelling in the growth plate after a single high dose of 5-FU. **A:** Nuclear BrdU-labelling (arrows) in some of the chondrocytes at the proliferative zone in a normal rat growth plate. **B:** Total suppression of BrdU labelling at the proliferative zone despite the presence of a positively labelled cell in the resting zone (arrow) on day 1 after 5-FU treatment. **C:** 5-FU treatment-induced changes in BrdU labelling index in the proliferative zone of growth plate. Bar in B = 25 μ m which applies to A. [Color figure can be viewed in the online issue, which is available at www.interscience.wiley.com.]

plate thickness by decreasing heights of both the proliferative and hypertrophic zones, the two zones that make up the bulk of the growth plate. In addition, counting the cells within cell columns revealed a similar pattern of decline and recovery in the numbers of chondrocytes residing in a column within the proliferative and hypertrophic zones (data not shown), suggesting that the changes in zonal heights

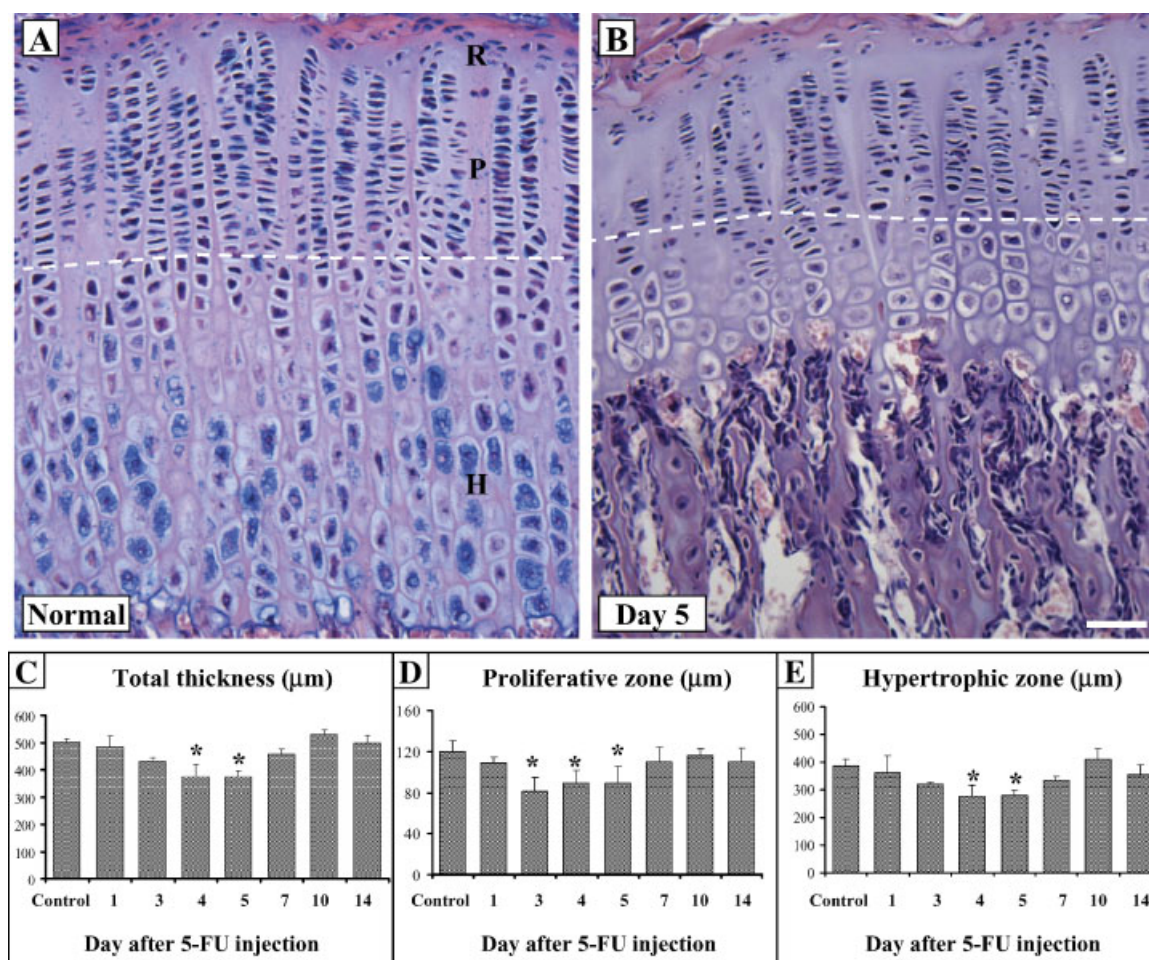


Fig. 4. Measurements of zonal heights in the growth plate after 5-FU acute treatment. **A:** A H&E-alcian blue stained section of a normal rat tibial growth plate (R, P and H denote resting, proliferative and hypertrophic zones, respectively; and dashed line represents a line drawn to separate the proliferative and hypertrophic zones). **B:** A H&E-alcian blue stained section of a rat

5 days after 5-FU treatment showing much thinner growth plate. **C:** Changes in measurements of the growth plate total thickness. **D:** Changes in the heights of the proliferative zone. **E:** Changes in the heights of the hypertrophic zone. Bar in B = 50 μm which applies to A. [Color figure can be viewed in the online issue, which is available at www.interscience.wiley.com.]

can be reflected by the changes in the number of cells per column at the two zones. The above results indicate that 5-FU-induced changes in growth plate thickness are caused by the alteration in the numbers of chondrocytes residing within the proliferative and hypertrophic zones.

Cellular and Histological Structural Changes in the Metaphysis

The metaphysis (adjacent to the growth plate) is responsible for converting calcified cartilage into trabecular bony tissue during bone lengthening. It has high levels of cell proliferation of pre-osteoblasts and osteoblasts and active bone formation and remodelling. In the current study, effects of 5-FU treatment on develop-

ment and recovery in apoptotic cell death, proliferation suppression and bone loss were examined in the metaphyseal bone within a 2-week time course.

Apoptosis in the metaphysis. At the primary spongiosa in the metaphysis, after 5-FU administration, there was a rapid induction in apoptotic cell death on days 1 and 2 among marrow cells, osteoblasts (lining the trabeculae) and preosteoblasts (located adjacent to the osteoblast layer in the primary spongiosa) as examined by H&E histology staining (Fig. 5B vs. A) and by TUNEL labelling (Fig. 5C). Apoptotic cell density measurements of osteoblasts and preosteoblasts on H&E stained sections (cells/mm^2) showed that the apoptotic rate in the metaphyseal primary spongiosa was

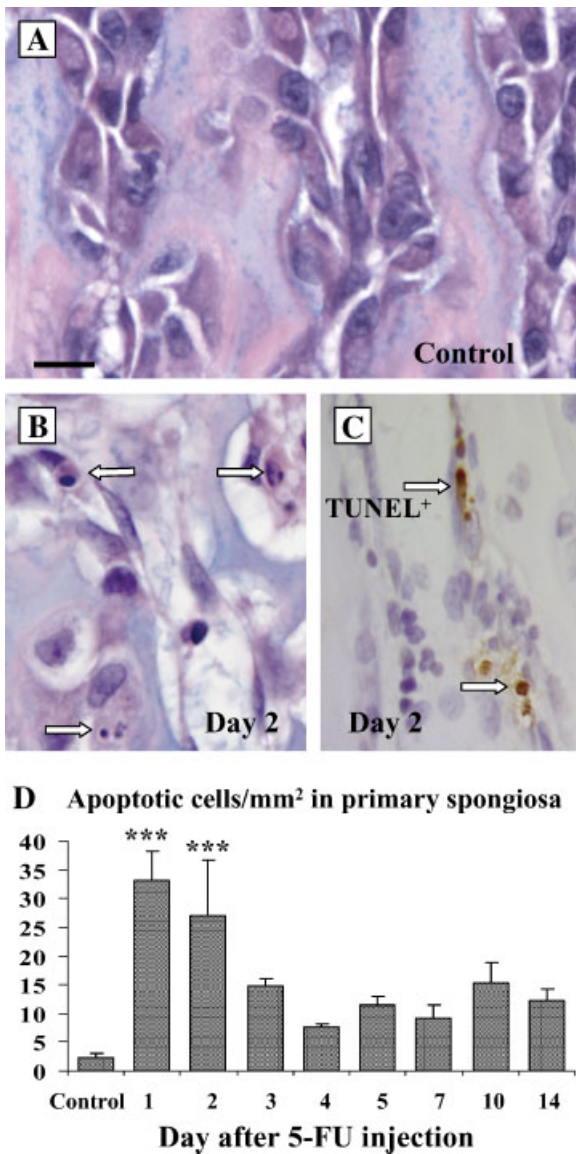


Fig. 5. Induction of apoptosis of osteoblasts and preosteoblasts at the metaphysis after a single high dose of 5-FU. **A:** A H&E-alcian blue stained section showing metaphyseal primary spongiosa in a normal rat. **B:** A H&E-alcian blue stained section showing apoptosis in osteoblasts or preosteoblasts (arrows) in metaphyseal primary spongiosa in a rat 2 days after 5-FU injection. **C:** A TUNEL-labelled section showing apoptosis in osteoblasts or preosteoblasts on or along the trabecular surface in metaphyseal primary spongiosa in a rat 2 days after 5-FU injection (arrows). **D:** Density measurements of total apoptotic osteoblasts and preosteoblasts per unit area of metaphyseal primary spongiosa. Bar in A = 25 μm (also applies to B and C). [Color figure can be viewed in the online issue, which is available at www.interscience.wiley.com.]

significantly up-regulated on days 1 and 2 ($P < 0.001$) compared to the basal level, and then declined to slightly but statistically insignificant higher levels than basal level on day 3 which persisted till day 14 (Fig. 5D).

Cell proliferation in the metaphysis. In the normal metaphysis, while BrdU labelling occurred mainly within the bone marrow among the osteoprogenitors and marrow cells, labelling was also located among osteoblasts lining the trabecular surface, and spindle-shaped preosteoblasts (located adjacent to osteoblast layer but without attachment to bone matrix as also demonstrated in previous studies [Turner et al., 1998; Xian et al., 2004a] (Fig. 6A). The number of BrdU-labelled osteoblasts and preosteoblasts per mm length of trabecular surface were 17 and 9 in the primary spongiosa (Fig. 6C,D), and 5 and 3 in the secondary spongiosa (Fig. 6E,F), respectively. After 5-FU treatment, on days 1 (Fig. 6B) and 2, the proliferation of osteoblasts and preosteoblasts were dramatically and significantly suppressed in both regions ($P < 0.001$) (Fig. 6C–F). However, starting from day 3 till day 14, the BrdU labelling index had returned to normal levels for both cell types in both regions.

Numbers of osteoblasts and preosteoblasts in the metaphysis. Consistent with the observations in the induction of apoptosis and suppression of cell proliferation early after 5-FU treatment, in the metaphyseal primary spongiosa, a single 5-FU injection significantly reduced the numbers of osteoblasts lining the trabecular surface (numbers of lining osteoblasts per mm trabecular surface perimeter) and adjacent spindle-shaped preosteoblasts along the trabecular surface on days 1–3, followed by a gradual recovery in the numbers of both osteoblasts and preosteoblasts which returned to normal levels by day 7 (Fig. 7A,B). In the secondary spongiosa, the numbers of lining osteoblasts were also significantly reduced during days 2–4 after 5-FU treatment, but those of the preosteoblasts did not change (Fig. 7C,D).

Histological structures in the metaphysis. Histology structures in the tibial long bone of normal rats and rats after 5-FU treatment were analysed at metaphyseal bone. There were time-dependent alterations in the heights, structure and projections of metaphyseal bone trabeculae, with the structural changes being most obvious from day 5 to 10 (Fig. 8C vs. B). However, by day 14, the metaphyseal trabecular structures (and the growth plate thickness) appeared to have returned to normal (Fig. 8D vs. A). Histological measurements in the metaphysis revealed a significant

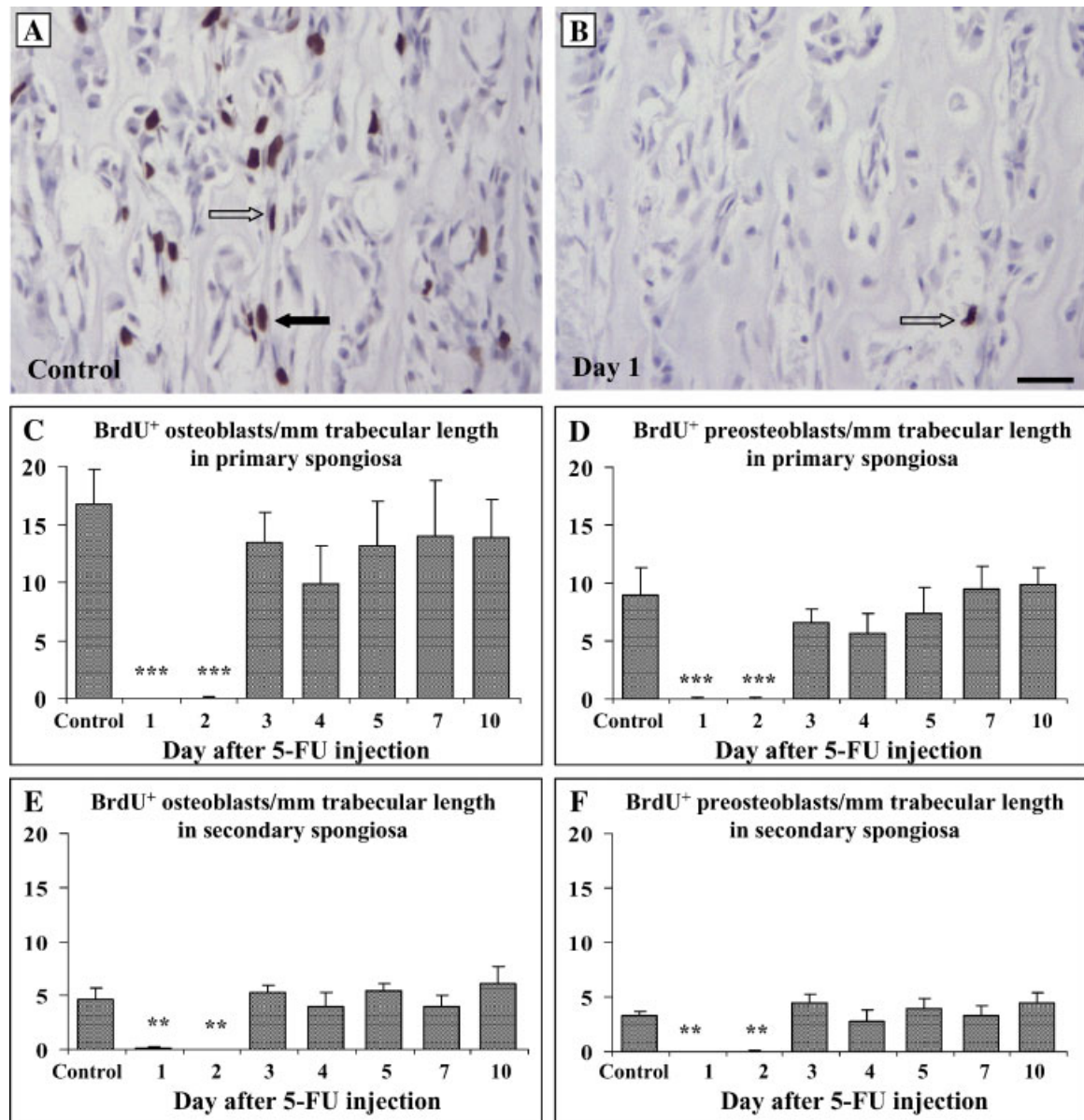


Fig. 6. Suppression and recovery of BrdU labelling in the metaphysis after a single high dose of 5-FU. **A:** Nuclear BrdU-labelling in some of the osteoblasts and preosteoblasts in the primary spongiosa of a normal rat, showing labelled osteoblasts (solid arrow) and preosteoblasts (block arrow). **B:** Total suppression of BrdU labelling among the osteoblasts and preosteoblasts at the primary spongiosa despite the presence of a positively labelled marrow cell (arrow) on day 1 after 5-FU treatment. (**C, D**)

5-FU treatment-induced changes in numbers of BrdU labelled osteoblasts (**C**) and preosteoblasts (**D**) per unit length of trabecular perimeter in the primary spongiosa. (**E, F**) 5-FU treatment-induced changes in numbers of BrdU labelled osteoblasts (**E**) and preosteoblasts (**F**) per unit length of trabecular perimeter in the secondary spongiosa. Bar in **B** = 25 μ m which applies to **A**. [Color figure can be viewed in the online issue, which is available at www.interscience.wiley.com.]

reduction in the height of primary spongiosa particularly during days 5–10 ($P < 0.01$), which returned to normal on day 14 (Fig. 9A). However, when the primary spongiosa histological structure was analysed horizontally, there were no significant changes observed ($P > 0.05$) in the trabecular numbers (Fig. 9C), thickness (average around 20 μ m, data not shown) and spacing

(Fig. 9E), as well as in the trabecular bone volume (Fig. 9G). On the other hand, in the secondary spongiosa, while the zonal height was not altered after 5-FU treatment (Fig. 9B) ($P > 0.05$), there were significant reductions in the trabecular bone volume (Fig. 9H) as there were significant decreases in the numbers of trabeculae (Fig. 9D) and increases in trabecular

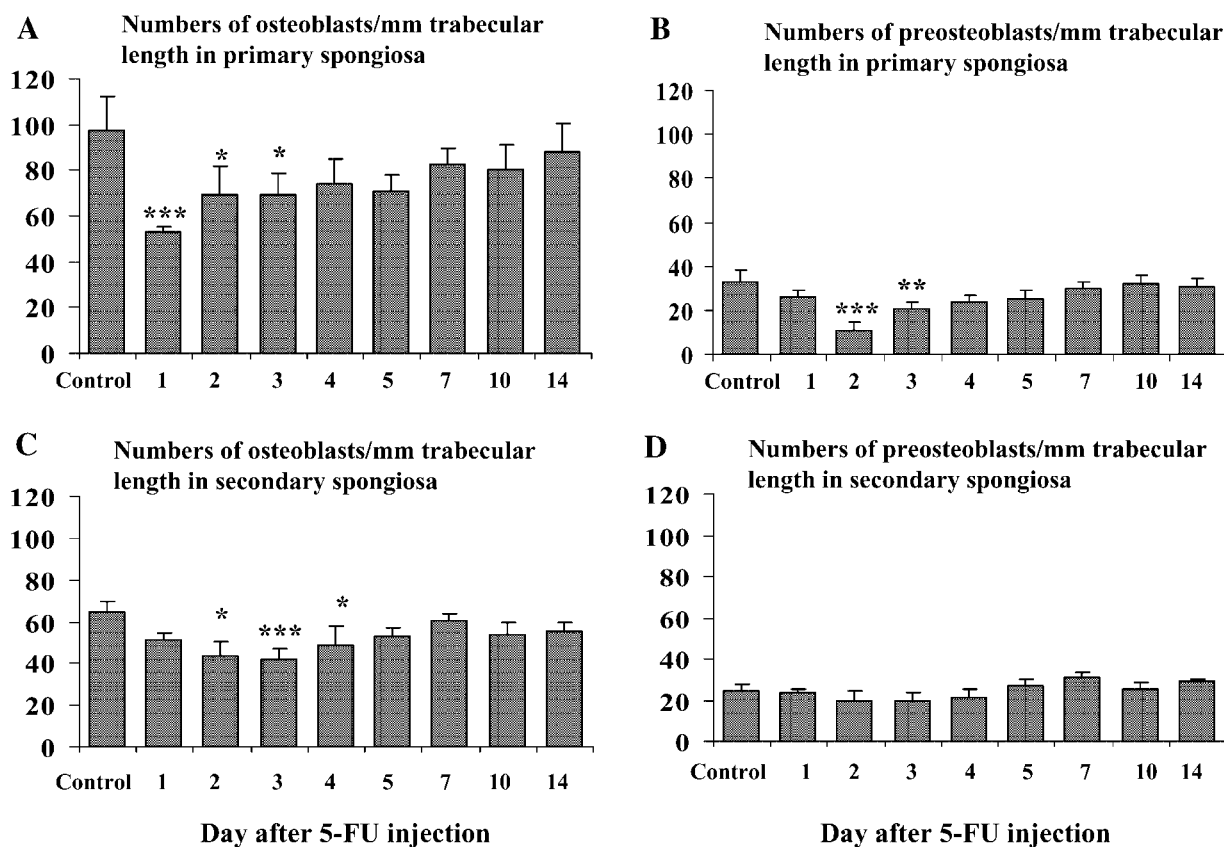


Fig. 7. Reduction and recovery of the osteoblast or preosteoblast cellularity in the metaphysis after a single high dose of 5-FU. (A, B) 5-FU treatment-induced changes in numbers of osteoblasts (A) and preosteoblasts (B) per unit length of trabecular perimeter in the primary spongiosa. (C, D) 5-FU treatment-induced changes in numbers of osteoblasts (C) and preosteoblasts (D) per unit length of trabecular perimeter in the secondary spongiosa.

spacing (Fig. 9F) during days 7–10 despite a lack of changes in the trabecular thickness (average around 40 μ m, data not shown).

Changes in Gene Expression in the Growth Plate and Metaphysis

As a step to investigate potential molecular mechanisms underlying the 5-FU-induced cellular and structural changes, analysis was made of effects of 5-FU treatment on mRNA expression of molecules known to be important in regulating apoptosis and proliferation as well as of matrix proteins. Since 5-FU-induced apoptosis of cancer cells can be initiated by mitochondrial dysfunction which is regulated by proapoptotic molecules such as Bax and antiapoptotic molecules such as Bcl-2 [Decaudin et al., 1998; Friesen et al., 1999; Tillman et al., 1999], relative expression levels of Bax and Bcl-2 were determined by quantitative real-time

RT-PCR in growth plate and metaphyseal bone RNA samples isolated from normal or 5-FU-treated rats. In the growth plate, interestingly, preceding the onset of apoptosis (apparent on day 5, peaking on day 7 and declining on day 10) (Fig. 2C), there was an obvious induction of *Bax* gene expression on days 1–4 followed by a decline and returning to normal levels during days 5–14 (Fig. 10A). Conversely, coinciding with the decline in apoptotic levels in the growth plate after 5-FU treatment, induction of Bcl-2 was apparent on day 5 and most obvious on day 10 (Fig. 10A). In the metaphysis, after 5-FU treatment, there was a significant upregulation in the expression of Bcl-2, and to a smaller extent, of Bax in days 3–10 during the recovery phase (Fig. 10B). Using the same RNA samples, expression levels were also determined for two important survival, mitogenic and differentiation factors, IGF-I and TGF- β 1. Analysis showed a larger induction of TGF- β 1 than

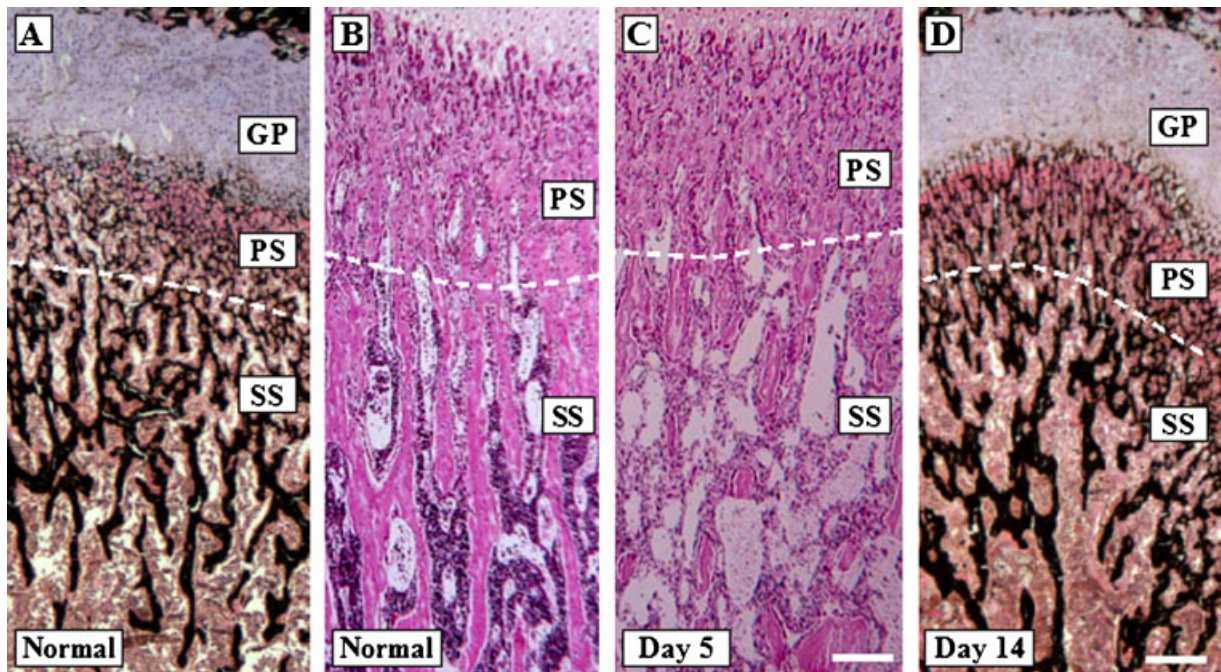


Fig. 8. Histological structural changes in the metaphyseal bone on day 5 and recovery on day 14 after a single high dose of 5-FU. (A, D) H&E and von Kossa stained undecalcified sections showing similar growth plate and metaphyseal bone structures in a normal rat (A) and a rat 14 days after 5-FU treatment (D). (B, C) H&E stained sections comparing metaphyseal bone

structures in a normal rat (B) and a rat 5 days after 5-FU treatment (C). Bar in C = 125 μm (also applies to B). Bar in D = 250 μm (also applies to A). GP, growth plate; PS, primary spongiosa; SS, secondary spongiosa. [Color figure can be viewed in the online issue, which is available at www.interscience.wiley.com.]

IGF-I, and a larger induction in the metaphyseal bone than in the growth plate, during the recovery phase after 5-FU treatment (Fig. 10C,D). Finally, after 5-FU treatment, upregulated expression of bone matrix proteins collagen-1 and osteocalcin was observed during the recovery phase on days 4–10 particularly day 7 (about 70 and 30 folds compared to normal levels, respectively) in the metaphyseal bone (Fig. 10F). In the growth plate, induction of cartilage proteins collagen-2a and collagen-10 was also observed on day 10 (about five-folds) (Fig. 10E). Interestingly, the expression levels of all genes analysed had returned to normal by day 14 (Fig. 10) when the growth plate and metaphysis recovered (Fig. 8D vs. A).

DISCUSSION

Intensive and long-term chemotherapy often causes bone growth arrest and development of osteoporosis in paediatric cancer patients or survivors. Consistent with *in vitro* studies showing adverse effects of chemotherapeutic drugs on proliferative capacity of cultured

growth plate chondrocytes [Robson et al., 1998] and osteoblasts and osteoblast precursor cells [Davies et al., 2002], our earlier *in vivo* study in young rats showed that a single injection of 5-FU caused rapid and significant suppression in cell proliferation in the growth plate and metaphysis and induction of apoptosis in the metaphysis on day 2 [Xian et al., 2004a]. Thus, this earlier study had provided *in vivo* evidence that 5-FU chemotherapy may impair the bone growth mechanisms directly to reduce longitudinal bone growth [Xian et al., 2004a]. To examine how well the bone growth mechanism can recover after a chemotherapy insult and to study potential molecular mechanisms underlying these changes, the current study characterised acute 5-FU treatment-induced development and resolution of the defects in growth plate and metaphysis. Using the same rat model, we have characterised the changes in apoptosis and proliferation of chondrocytes, osteoblasts and preosteoblasts, changes in their histological structures, and alteration in expression of matrix molecules and some genes known to be important in regulating the cellular

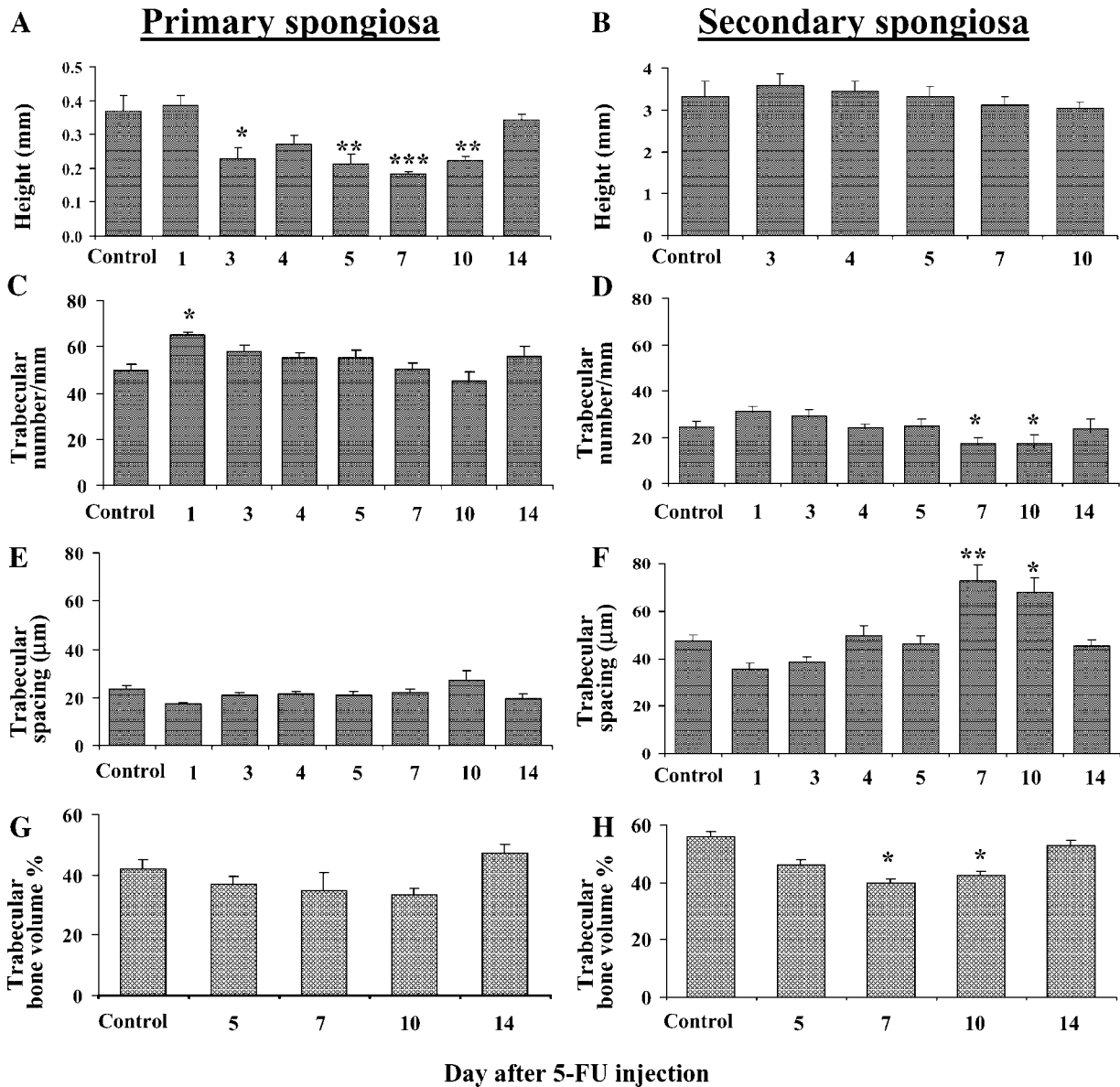


Fig. 9. Trabecular bone structural changes in the primary spongiosa (A, C, E, G) and secondary spongiosa (B, D, F, H) in the metaphysis after a single high dose of 5-FU. (A, B) Zonal heights of primary or secondary spongiosa in a longitudinal plane. (C, D) Average numbers of bony trabeculae per unit width of metaphysis on a cross plane. (E, F) Average spacing of (or distance between) bony trabeculae on a cross plane. (G, H) Average bone volume % of bony trabeculae (i.e., % of trabecular bone area over total tissue area).

processes in these two important tissues for bone growth.

In the current study, we have demonstrated that a single high dose of 5-FU caused a rapid induction of apoptosis of osteoblasts and preosteoblasts in the metaphysis on days 1–2, which declined thereafter. Interestingly, apoptosis among proliferative chondrocytes was somewhat delayed and not seen until during days 5–10 and disappeared by day 14. In

addition, 5-FU not only induced apoptosis, it rapidly and dramatically suppressed proliferation of chondrocytes in the growth plate and osteoblasts and preosteoblasts in the metaphysis, with a total suppression in BrdU labelling seen on days 1 and 2. Interestingly, the recovery time course in BrdU labelling was different in the growth plate and metaphysis. While the BrdU labelling had a full recovery starting on day 3 in the metaphysis, in the growth plate, it

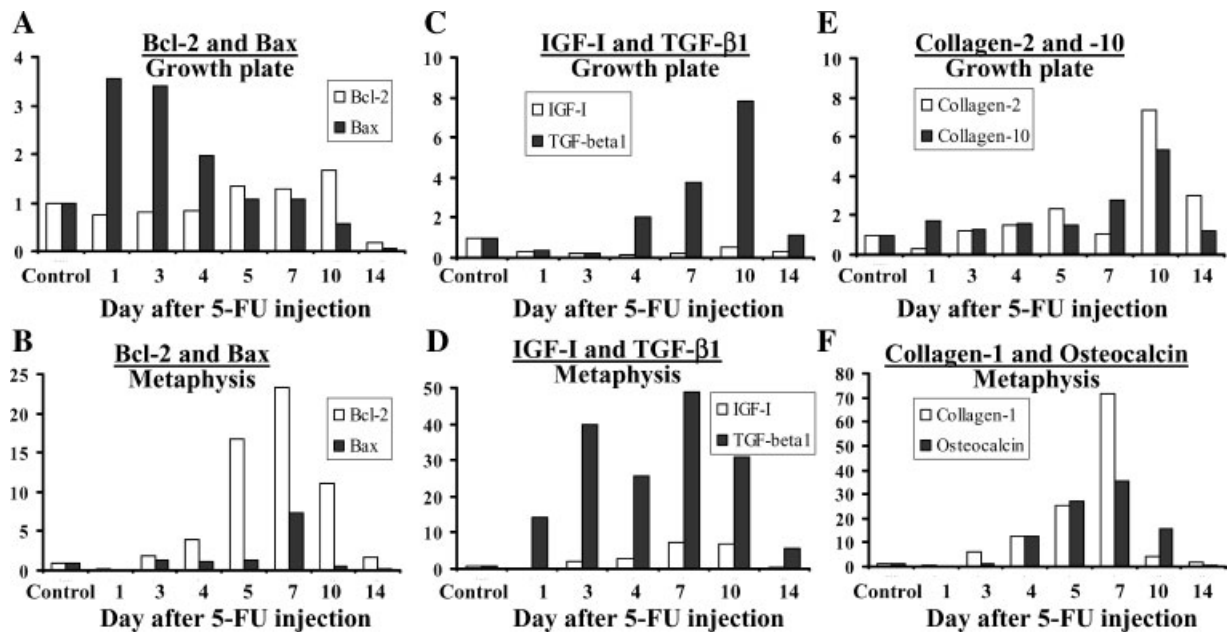


Fig. 10. Changes in mRNA expression of (A, B) apoptosis-regulatory molecules (Bax and Bcl-2), (C, D) growth factors (IGF-I and TGF- β 1) and (E, F) matrix proteins (collagen-2, collagen-10, collagen-1 and osteocalcin) in the proximal tibial growth plate and metaphysis after a single high dose 5-FU injection in young rats. Relative expression levels are presented as fold change in relation to the normal control. Real time RT-PCR assays were conducted from pooled RNA samples, with each RNA pool derived from six animals per group.

partially recovered on day 3 and then overshoot to levels slightly higher than normal on days 5 and 7 before returning to the basal level on day 10.

It remains to be investigated why the temporal patterns in the development and resolution in 5-FU-induced changes in apoptosis and proliferation are somewhat different between growth plate and metaphysis. However, these time course differences in cellular damage and recovery seen could potentially be related with the extents of vascularisation within the tissues. While the growth plate is relatively avascular with access to nutrients or drugs occurring via diffusion only (from the terminals of epiphyseal artery), the metaphysis is well vascularised (by nutrient artery and metaphyseal artery). In addition, it is known that 5-FU-induced cellular damage can be initiated via different mechanisms depending on tissue or cell types [Decaudin et al., 1998; Friesen et al., 1999; Tillman et al., 1999]. Interestingly, our gene expression analysis has demonstrated that upregulation of pro-apoptotic molecule Bax preceded the onset of apoptosis and the increased expression of anti-apoptotic molecule Bcl-2 occurred during the repair phase in the

growth plate. In the metaphysis, Bcl-2, and to a smaller extent, Bax, were seen upregulated during the repair phase. These findings suggest that the Bax/Bcl-2 signalling pathway is involved in regulating the 5-FU-induced apoptosis in growth plate chondrocytes and metaphyseal bone osteoblasts and preosteoblasts.

In the present study, we have shown that the significant effects of 5-FU on cell proliferation and apoptosis resulted in a significant reduction of cellularity in both the proliferative and hypertrophic zones and thus a reduction in the thickness of the growth plate. In addition, since the primary spongiosa region of the metaphyseal bone is directly derived from the growth plate, it is not surprising that the reduced growth plate width (during days 3–5) is also reflected by a decreased height of the primary spongiosa which occurred during days 5–10. Similarly, consistent with the significant effects on cell proliferation and apoptosis in the metaphysis seen early after 5-FU treatment, a considerable reduction of the numbers of osteoblasts and preosteoblasts on or along the trabecular bone surface was also observed on days 1–3 after 5-FU administration. However, despite these changes in bone cell numbers,

there were no obvious changes seen in the number of bony trabeculae, their thickness and spacing and correspondingly no changes in the trabecular bone area percentage in the primary spongiosa. On the other hand, in the secondary spongiosa which houses bony trabeculae further remodelled from those in the primary spongiosa, there was a significant reduction in the bone area on days 7 and 10, which was shown to be related to reduced number of bony trabeculae and increased spacing between them on days 5–7 after 5-FU treatment. Since there were no obvious changes in the osteoclast density (numbers of osteoclasts per unit length of trabecular perimeter) observed in both primary and secondary spongiosa (data not shown), the reduced bone volume in days 7 and 10 in the secondary spongiosa could be most likely culminated from reduced number of osteoblasts early after 5-FU treatment in both primary and secondary spongiosa. Previous studies using young rats found that administration of doxorubicin or methotrexate at a clinical therapeutic dosage for a short term (5 days) significantly reduced the trabecular bone volume in the tail vertebrae [Friedlander et al., 1984].

Previous studies have suggested that as long as the stem cells are not completely destroyed by the chemotherapy, damaged tissues such as the intestinal mucosa with chemotherapy-induced damage (“mucositis”) can regenerate after the insult [Houchen et al., 1999; Booth and Potten, 2001; Xian, 2003]. In the current study, in contrast to the obvious changes seen in the proliferative zone of the growth plate, there were no apparent changes observed in the resting zone of the growth plate, a region which houses the progenitor cells of the growth plate. Consistently, recovery of the growth plate in cellular proliferative activity and histological structure was seen by days 10 or 14 after 5-FU treatment. Interestingly, increased mRNA expression of growth factor TGF- β 1 and growth plate cartilage matrix proteins collagen-2 and collagen-10 was observed during the recovery phase which returned to normal levels by day 14, further suggesting the growth plate can recover after 5-FU acute chemotherapy.

In the metaphysis, the bony trabeculae in the primary spongiosa are derived from the growth plate trabeculae and are destined to be further remodelled to become the more mature bone trabeculae in the secondary spongiosa through

action of resorptive cells osteoclasts and bone synthesizing cells osteoblasts. Therefore, mirroring the recovery time course of the growth plate width, the time-dependent recuperation of the primary spongiosa height was observed in the present study. Since the osteoclast density in the metaphysis was not affected, repair of the secondary spongiosa in the metaphysis was most likely resulted from the recovery of the osteoblasts and their synthetic activity. Interestingly, during the recovery of the metaphysis, there was a significant upregulation of bone matrix proteins collagen-1 and osteocalcin and growth factors TGF- β 1 and IGF-I. These two growth factors are known to be important in bone cell recruitment, proliferation, differentiation and bone formation [Price et al., 1994; Rosier et al., 1998; McCarthy and Centrella, 2001; Yakar and Rosen, 2003]. In the current study, recovery of the proliferative activity and their total numbers of both osteoblasts and preosteoblasts was observed starting from day 4 after 5-FU treatment. Significant upregulation of bone matrix proteins (collagen-1 and osteocalcin) during days 4 and 10 suggest that after the osteoblasts and preosteoblasts had recovered to normal in density by day 4, they significantly increased their bone formation activity for the bone recovery. By day 14, cells numbers, levels of gene expression and histological structure of the metaphysis returned to normal.

In our current study, our experimental animals had been given a single high dose of 5-FU at 150 mg/kg, which is a commonly used dose in rats [Hopkins et al., 1976] and is equivalent to 817 mg/m² body area surface based on dosage conversion for rats [van Leeuwen et al., 2000a]. Although this single dose of 5-FU significantly reduce the gain of total body length by 2 weeks, when examining the effects on tibial long bone alone, this single-dose was shown not to significantly affect the tibial bone lengthening within the 2-week observation period despite the significant effects observed on cellular activity and histological structures. Further studies are required to study whether a long term 5-FU chemotherapy in a therapeutic dose would reduce bone linear growth (e.g., at the equivalent recommended individual bolus dose for adult human at 450 mg/m²/day for 5 days followed by a maintenance therapy at a lower dose). Previous experimental studies using young rats have found that administration of

doxorubicin or methotrexate at a clinical therapeutic dosage for 8 weeks, longitudinal growth of the tibia was reduced by 18% and 5% respectively [van Leeuwen et al., 2000a].

Taken together, the present study has demonstrated that a single high dose of 5-FU significantly suppressed cell proliferation and induced apoptosis in both growth plate and metaphysis, resulting in a thinner growth plate, a thinner primary spongiosa and an osteopenic condition in the secondary spongiosa. These findings suggest that 5-FU can block cell proliferation and induce apoptosis in both growth plate and metaphysis, two most important tissues responsible for bone growth in children. In addition, the current study has also shown that, after the 5-FU acute treatment, the cellular activities and histological structure can recover and return to normal states by day 10 or day 14, and that the recovery process is associated with significant upregulation of mRNA expression of matrix proteins, growth factors and apoptosis-regulatory molecules.

ACKNOWLEDGMENTS

The authors thank Mark Covino and Carmen Macsai for some technical assistance.

REFERENCES

- Ahmed SF, Wallace WH, Kelnar CJ. 1997. An anthropometric study of children during intensive chemotherapy for acute lymphoblastic leukaemia. *Horm Res* 48:178–183.
- Ahmed SF, Wallace WH, Crofton PM, Wardhaugh B, Magowan R, Kelnar CJ. 1999. Short-term changes in lower leg length in children treated for acute lymphoblastic leukaemia. *J Pediatr Endocrinol Metab* 12:75–80.
- Angel CA, Pratt CB, Rao BN, Schell MJ, Parham DM, Lobe TE, Fleming ID. 1992. Carcinoembryonic antigen and carbohydrate 19-9 antigen as markers for colorectal carcinoma in children and adolescents. *Cancer* 69:1487–1491.
- Beresford JN. 1989. Osteogenic stem cells and the stromal system of bone and marrow. *Clin Orthop* 240:278–280.
- Booth D, Potten CS. 2001. Protection against mucosal injury by growth factors and cytokines. *J Natl Cancer Inst Monogr* 29:16–20.
- Byers S, Moore AJ, Byard RW, Fazzalari NL. 2000. Quantitative histomorphometric analysis of the human growth plate from birth to adolescence. *Bone* 27:495–501.
- Caruso-Nicoletti M, Mancuso M, Spadaro G, Dibenedetto SP, DiCataldo A, Schiliro G. 1993. Growth and growth hormone in children during and after therapy for acute lymphoblastic leukaemia. *Eur J Pediatr* 152:730–733.
- Clayton PE, Shalet SM, Morris-Jones PH, Price DA. 1988. Growth in children treated for acute lymphoblastic leukaemia. *Lancet* 1:460–462.
- Cool JC, Dyer JL, Xian CJ, Butler RN, Geier MS, Howarth GS. 2005. Pre-treatment with insulin-like growth factor-I partially ameliorates 5-fluorouracil-induced intestinal mucositis in rats. *Growth Horm IGF Res* 15:72–82.
- Crofton PM, Ahmed SF, Wade JC, Stephen R, Elmlinger MW, Ranke MB, Kelnar CJ, Wallace WH. 1998. Effects of intensive chemotherapy on bone and collagen turnover and the growth hormone axis in children with acute lymphoblastic leukemia. *J Clin Endocrinol Metab* 83:3121–3129.
- Damron TA, Margulies BS, Strauss JA, O'Hara K, Spadaro JA, Farnum CE. 2003. Sequential histomorphometric analysis of the growth plate following irradiation with and without radioprotection. *J Bone Joint Surg Am* 85-A:1302–1313.
- Davies JH, Evans BA, Jenney ME, Gregory JW. 2002. In vitro effects of combination chemotherapy on osteoblasts: Implications for osteopenia in childhood malignancy. *Bone* 31:319–326.
- Decaudin D, Marzo I, Brenner C, Kroemer G. 1998. Mitochondria in chemotherapy-induced apoptosis: A prospective novel target of cancer therapy (review). *Int J Oncol* 12:141–152.
- Fazzalari NL, Moore AJ, Byers S, Byard RW. 1997. Quantitative analysis of trabecular morphogenesis in the human costochondral junction during the postnatal period in normal subjects. *Anat Rec* 248:1–12.
- Friedlander GE, Tross RB, Doganis AC, Kirkwood JM, Baron R. 1984. Effects of chemotherapeutic agents on bone: Short-term methotrexate and doxorubicin treatment in a rat model. *J Bone Joint Surg* 66A:602–607.
- Friesen C, Fulda S, Debatin KM. 1999. Cytotoxic drugs and the CD95 pathway. *Leukemia* 13:1854–1858.
- Glasser DB, Duane K, Lane JM, Heuley JH, Caparros-Sison B. 1991. The effect of chemotherapy on growth in the skeletally immature individual. *Clin Orthop* 262:93–100.
- Halton JM, Atkinson SA, Fraher L, Webber C, Gill GJ, Dawson S, Barr RD. 1996. Altered mineral metabolism and bone mass in children during treatment for acute lymphoblastic leukemia. *J Bone Miner Res* 11:1774–1783.
- Halton JM, Atkinson SA, Barr RD. 1998. Growth and body composition in response to chemotherapy in children with acute lymphoblastic leukemia. *Int J Cancer Suppl* 11:81–84.
- Hopkins HA, Kovacs CJ, Looney WB, Wakefield JA. 1976. Differential recovery of intestine, bone marrow, and thymus of rats with solid tumors following 5-fluorouracil administration. *Cancer Biochem Biophys* 1:303–312.
- Hoshi K, Amizuka N, Oda K, Ikehara Y, Ozawa H. 1997. Immunolocalization of tissue non-specific alkaline phosphatase in mice. *Histochem Cell Biol* 107:183–191.
- Houchen CW, George RJ, Sturmoski MA, Cohn SM. 1999. FGF-2 enhances intestinal stem cell survival and its expression is induced after radiation injury. *Am J Physiol* 276:G249–G258.
- Ianotti JP. 1990. Growth plate physiology and pathology. *Orthop Clin N Am* 21:1–17.
- Katzenstein HM, Krailo MD, Malogolowkin MH, Ortega JA, Qu W, Douglass EC, Feusner JH, Reynolds M,

- Quinn JJ, Newman K, Finegold MJ, Haas JE, Sensel MG, Castleberry RP, Bowman LC. 2003. Fibrolamellar hepatocellular carcinoma in children and adolescents. *Cancer* 97:2006–2012.
- Kember NF. 1993. Cell kinetics and the control of bone growth. *Acta Paediatr Suppl* 82(Suppl 391):61–65.
- Kim TH, McLaren J, Alvarado CS, Wylly JB, Crocker I, Winn K, Singhapakdi S, Ragab A. 1989. Adjuvant chemotherapy for advanced nasopharyngeal carcinoma in childhood. *Cancer* 63:1922–1926.
- Linnet MS, Ries LAG, Smith MA, Tarone RE, Devesa SS. 1999. Recent trends in childhood cancer incidence and mortality in the United States. *J Natl Cancer Inst* 91:1051–1058.
- Liu W, Saint DA. 2002. Validation of a quantitative method for real time PCR kinetics. *Biochem Biophys Res Commun* 294:347–353.
- Long MW. 2001. Osteogenesis and bone-marrow-derived cells. *Blood Cells Mol Dis* 27:677–690.
- Longley DB, Harkin DP, Johnston PG. 2003. 5-fluorouracil: Mechanisms of action and clinical strategies. *Nat Rev Cancer* 3:330–338.
- Marks SC, Jr. 1998. Osteoclast biology: Lessons from mammalian mutations. *Am J Med Genet* 34:43–54.
- McCarthy TL, Centrella M. 2001. Local IGF-I expression and bone formation. *Growth Horm IGF Res* 11:213–219.
- Mushtaq T, Ahmed SF. 2002. The impact of corticosteroids on growth and bone health. *Arch Dis Child* 87:93–96.
- Peters GJ, van der Wilt CL, van Moorsel CJA, Kroep JR, Bergman AM, Ackland SP. 2000. Basis for effective combination cancer chemotherapy with antimetabolites. *Pharmacol Ther* 87:227–253.
- Price JS, Oyajobi BO, Russell RG. 1994. The cell biology of bone growth. *Eur J Clin Nutr* 48(Suppl 1):S131–S149.
- Robson H, Anderson E, Eden OB, Isaksson O, Shaler SM. 1998. Chemotherapeutic agents used in the treatment of childhood malignancies have direct effects on growth plate chondrocyte proliferation. *J Endocrinol* 157:225–235.
- Rosier RN, O'Keefe RJ, Hicks DG. 1998. The potential role of transforming growth factor beta in fracture healing. *Clin Orthop Relat Res* 355(Suppl):S294–S300.
- Saade M, Debahy NE, Houjeily S. 1999. Clinical remission of xeroderma pigmentosum-associated squamous cell carcinoma with isotretinoin and chemotherapy: Case report. *J Chemother* 11:313–317.
- Samuelsson BO, Marky I, Rosberg S, Albertsson-Wikland K. 1997. Growth and growth hormone secretion after treatment for childhood non-Hodgkin's lymphoma. *Med Pediatr Oncol* 28:27–34.
- Sanchez CP, He YZ. 2002. Alterations in the growth plate cartilage of rats with renal failure receiving corticosteroid therapy. *Bone* 30:692–698.
- Sasaki H, Sasano H, Ohi R, Imaizumi M, Shineha R, Nakamura M, Shibuya D, Hayashi Y. 1999. Adenocarcinoma at the esophageal gastric junction arising in an 11-year-old girl. *Pathol Int* 49:1109–1113.
- Schriock EA, Schell MJ, Carter M, Hustu O, Ochs JJ. 1991. Abnormal growth patterns and adult short stature in 115 long-term survivors of childhood leukemia. *J Clin Oncol* 9:400–405.
- Siebler T, Shalet SM, Robson H. 2002. Effects of chemotherapy on bone metabolism and skeletal growth. *Horm Res* 58(Suppl 1):80–85.
- Sims NA, Clement-Lacroix P, Da Ponte F, Bouali Y, Binart N, Moriggl R, Goffin V, Coschigano K, Gaillard-Kelly M, Kopchick J, Baron R, Kelly PA. 2000. Bone homeostasis in growth hormone receptor-null mice is restored by IGF-I but independent of Stat5. *J Clin Invest* 106:1095–1103.
- Snir M, Lusky M, Shalev B, Gatot D, Weinberger D. 2000. Mitomycin C and 5-fluorouracil antimetabolite therapy for pediatric glaucoma filtration surgery. *Ophthalmic Surg Lasers* 31:31–37.
- Tillman DM, Petak I, Houghton JA. 1999. A Fas-dependent component in 5-fluorouracil/leucovorin-induced cytotoxicity in colon carcinoma cells. *Clin Cancer Res* 5:425–430.
- Turner CH, Owan I, Alvey T, Hulman J, Hock JM. 1998. Recruitment and proliferative responses of osteoblasts after mechanical loading in vivo determined using sustained-release bromodeoxyuridine. *Bone* 22:463–469.
- van Leeuwen BL, Kamps WA, Hartel RM, Veth RP, Sluiter WJ, Hoekstra HJ. 2000a. Effect of single chemotherapeutic agents on the growth skeleton of the rat. *Ann Oncol* 11:1121–1126.
- van Leeuwen BL, Kamps WA, Jansen HW, Hoekstra HJ. 2000b. The effect of chemotherapy on the growing skeleton. *Cancer Treat Rev* 26:363–376.
- Xian CJ. 2003. Roles of growth factors in chemotherapy-induced intestinal mucosal damage repair. *Curr Pharm Biotechnol* 4:260–269.
- Xian CJ, Howarth GS, Mardell CE, Cool JC, Familiari M, Read LC, Giraud AS. 1999. Temporal changes in TFF3 expression and jejunal morphology during methotrexate-induced damage and repair. *Am J Physiol* 277:G785–G795.
- Xian CJ, Cool JC, Howarth GS, Read LC. 2002. Effects of TGF- α gene knockout on epithelial cell kinetics and repair of methotrexate-induced damage in mouse small intestine. *J Cell Physiol* 191:105–115.
- Xian CJ, Howarth GS, Cool J, Foster BK. 2004a. Effects of acute 5-fluorouracil chemotherapy and insulin-like growth factor-I pretreatment on growth plate cartilage and metaphyseal bone in rats. *Bone* 35:739–749.
- Xian CJ, Zhou FH, McCarty RC, Foster BK. 2004b. Intramembranous ossification mechanism for bone bridge formation at the growth plate cartilage injury site. *J Orthop Res* 22:417–426.
- Yakar S, Rosen CJ. 2003. From mouse to man: Redefining the role of insulin-like growth factor-I in the acquisition of bone mass. *Exp Biol Med (Maywood)* 228:245–252.
- Zhou FH, Foster BK, Sander G, Xian CJ. 2004. Expression of proinflammatory cytokines and growth factors at the injured growth plate cartilage in young rats. *Bone* 35:1307–1315.
- Zidan J, Kuten A, Rosenblatt E, Robinson E. 1997. Intensive chemotherapy using cisplatin and fluorouracil followed by radiotherapy in advanced head and neck cancer. *Oral Oncol* 33:129–135.